2018

Experimental Investigation on the Effect of Corrosion on the Bond Between Reinforcing Steel Bars and Fibre Reinforced Geopolymer Concrete

Nabeel Farhan
University of Wollongong, naf010@uowmail.edu.au

M Neaz Sheikh
University of Wollongong, msheikh@uow.edu.au

Muhammad N. S Hadi
University of Wollongong, mhadi@uow.edu.au

Experimental Investigation on the Effect of Corrosion on the Bond Between Reinforcing Steel Bars and Fibre Reinforced Geopolymer Concrete

Abstract

This paper investigates the effect of corrosion on the bond between reinforcing steel bars and fibre reinforced geopolymer concrete. An accelerated corrosion method was used to corrode the reinforcing steel bars embedded in geopolymer concrete. Three types of steel fibres including straight micro steel fibre, deformed macro steel fibre, and hybrid steel fibre were used in this study. A total of ten geopolymer concrete mixes were used to evaluate the effect of corrosion of steel bar on the bond between steel bar and fibre reinforced geopolymer concrete. The pull-out test specimens were composed of concrete cubes with a side length of 160mm and reinforced with a deformed steel bar of 16 mm diameter located at the centre of the specimens. The test results showed that the addition of steel fibres in geopolymer concrete (fibre reinforced geopolymer concrete) significantly enhanced the bond strength of reinforcing steel bar. The bond strength of reinforcing steel bars embedded in steel fibre reinforced geopolymer concrete specimens reduced due to corrosion of reinforcement. However, the reduction of bond strength in steel fibre reinforced geopolymer concrete specimens was less than the reduction of bond strength in plain geopolymer concrete specimen.

Disciplines

Engineering | Science and Technology Studies

Publication Details

Farhan, N. A., Sheikh, M. Neaz. & Hadi, M. N. S. (2018). Experimental Investigation on the Effect of Corrosion on the Bond Between Reinforcing Steel Bars and Fibre Reinforced Geopolymer Concrete. Structures, 14 251-261.

Experimental Investigation on the Effect of Corrosion on the Bond between Reinforcing Steel Bars and Fibre Reinforced Geopolymer Concrete

Nabeel A. Farhan[1], M. Neaz Sheikh[2], Muhammad N.S. Hadi[3*],

[1] Ph.D. Candidate, School of Civil, Mining and Environmental Engineering, University of Wollongong, Australia

[2] Associate Professor, School of Civil, Mining and Environmental Engineering, University of Wollongong, Australia

[3*] Associate Professor, School of Civil, Mining and Environmental Engineering, University of Wollongong, Australia

Correspondence:

Muhammad N. S. Hadi

School of Civil, Mining & Environmental Engineering

University of Wollongong, Australia

E-mail: mhadi@uow.edu.au

Telephone: + 61 2 4221 4762

Facsimiles: + 61 2 4221 3238

---

* Corresponding author

Experimental Investigation on the Effect of Corrosion on the Bond between Reinforcing Steel Bars and Fibre Reinforced Geopolymer Concrete

Abstract

This paper investigates the effect of corrosion on the bond between reinforcing steel bars and fibre reinforced geopolymer concrete. An accelerated corrosion method was used to corrode the reinforcing steel bars embedded in geopolymer concrete. Three types of steel fibres including straight micro steel fibre, deformed macro steel fibre, and hybrid steel fibre were used in this study. A total of ten geopolymer concrete mixes were used to evaluate the effect of corrosion of steel bar on the bond between steel bar and fibre reinforced geopolymer concrete. The pull-out test specimens were composed of concrete cubes with a side length of 160 mm and reinforced with a deformed steel bar of 16 mm diameter located at the centre of the specimens. The test results showed that the addition of steel fibres in geopolymer concrete (fibre reinforced geopolymer concrete) significantly enhanced the bond strength of reinforcing steel bar. The bond strength of reinforcing steel bars embedded in steel fibre reinforced geopolymer concrete specimens reduced due to corrosion of reinforcement. However, the reduction of bond strength in steel fibre reinforced geopolymer concrete specimens was less than the reduction of bond strength in plain geopolymer concrete specimen.

Keywords: Corrosion; Bond; Geopolymer; Steel Fibres; Pull-out

1. Introduction

The process of the production of cement is associated with high energy consumption causing adverse environmental impact. It was estimated that the production of one tonne of cement requires about one tonne of raw materials and emits nearly one tonne of carbon dioxide (CO_2) into the atmosphere [1-3]. Hence, to reduce the adverse environmental impact associated with the production of cement, the use of alternative binders to cement such as industrial by-products are considered an attractive solution to reduce or alleviate adverse environmental impacts. During the last few decades, research investigations were carried out into the use of geopolymer concrete as an alternative to the Ordinary Portland Cement (OPC) concrete.

Geopolymer concrete consumes lower energy and causes low carbon dioxide emissions into the atmosphere. It possesses high early strength, high fire resistance and high durability against chemical attack. It has been a promising material to be used in different construction applications as an alternative to OPC concrete [4-7]. On the other hand, low tensile and flexural strengths are the main drawbacks limiting the use of geopolymer concrete in several applications including the construction of columns and beams. The addition of steel fibres was found to be a promising solution to enhance the tensile and flexural strengths of geopolymer concrete [8]. Ng et al. [9] found that shear strength of geopolymer concrete beams increased with the addition of steel fibre. Bernal et al. [10] investigated the mechanical properties and durability performance of heat cured geopolymer concrete reinforced with various proportions of steel fibre ranging from 0 to 3% by volume. The test results showed a reduction of the compressive strength with the addition of steel fibres. However, splitting tensile strength and flexural strength were significantly improved with the increase in the addition of steel fibres from 0 to 3% by volume. Also, the durability performances including

72 water absorption, capillarity and water penetration resistance were enhanced with the addition
73 steel fibres in the heat cured geopolymer concrete [10].

74 A large number of reinforced concrete structures are exposed to chloride attack leading to the
75 corrosion of reinforcing steel bars [11]. The corrosion of the steel bar has significant adverse
76 effects on the durability and serviceability of the reinforced concrete (RC) structures [12].
77 Several research studies reported that the corrosion of the steel bar in RC structures reduced
78 the tensile strength of the reinforcing bars because of the loss of the cross-sectional area and
79 loss in the bond performance between reinforcing steel bar and surrounding concrete [13, 14].
80 Abosrra et al. [15] studied the effect of corrosion on the bond behaviour of deformed steel
81 bars embedded in concrete with different compressive strengths. The test results showed that
82 higher compressive strength of concrete increased the bond strength and reduced the rate of
83 corrosion of steel reinforcing bar.

84 Steel fibres are commonly used for reinforcing the precast elements, hydraulic structures,
85 airfield pavements, and tunnel lining segments. However, steel fibres cannot be used to
86 replace the conventional reinforcing steel bars in most concrete members. Steel fibres are
87 used as complementary to the conventional reinforcing steel bars in RC structures. However,
88 some studies recommended for not using steel fibre in combination with conventional
89 reinforcing steel bars in saltwater environments because of the concerns that steel fibres
90 might accelerate the corrosion of reinforcing steel bars in RC structures [16, 17].

91 Roque et al. [18] studied the durability of hooked end steel fibre of RC structural members.
92 The test results showed that steel fibres improved the durability of RC structures in non-
93 submerged saltwater environments. It was recommended that steel fibres should not be used
94 in combination with reinforcing steel bars in seawater environments because steel fibres in
95 contact with reinforcing steel bars accelerated the corrosion of the reinforcing steel bars [18].

Grubb et al. [19] investigated the effect of micro steel fibres on the corrosion of reinforcing steel bars. Mortar specimens with and without micro steel fibres were exposed to a corrosive environment. Steel bars embedded in mortar reinforced with micro steel fibres showed better resistance to corrosion than steel bars embedded in plain mortar. Someh and Saeki [20] studied the durability of concrete reinforced by zinc-coated steel fibres. Steel bars embedded in zinc-coated steel fibre reinforced concrete remained free from corrosion for a longer period of time compared to steel bar embedded in plain concrete when exposed to similar corrosive environments.

Sofi et al. [21] investigated the bond strength of geopolymer concrete with reinforcing steel bar. The test results showed that all specimens failed by splitting of geopolymer concrete surrounding the steel bar and the bond strength increased with a decrease in the diameter of the reinforcing steel bar. The bond strength of geopolymer concrete and OPC concrete with reinforcing steel bars was also studied by Sarker [22]. The test results showed that both geopolymer concrete and OPC concrete specimens failed by splitting of concrete around the region bonded with the reinforcing steel bar. The test results also showed that geopolymer concrete had higher bond strength than OPC concrete with reinforcing steel bars [22]. Castel and Foster [23] also reported that the bond strength of reinforcing steel bar embedded in the geopolymer concrete was slightly higher than the bond strength of reinforcing steel bar embedded in the OPC concrete.

Different test methods were adopted in the previous research studies for measuring the bond between reinforcing steel bars and concrete including pull-out test [21], beam end test [22], beam anchorage test [24] and splice test [25]. In this study, the pull-out test was used because of the ease of fabrication and the simplicity of the test. Several research studies investigated the bond of reinforcing steel bars embedded in geopolymer concrete. However, the effect of

corrosion on the bond performance of reinforcing steel bars embedded in steel fibre reinforced geopolymer concrete has not yet been investigated. The objective of this study, therefore, is to evaluate the effect of corrosion on the bond between steel bars and fibre reinforced geopolymer concrete. The objective of this study is achieved through extensive experimental investigations. The development of a mathematical model is considered beyond the scope of this paper.

2. Experimental program

2.1 Materials

The materials used in this study included ground granulated blast furnace slag (GGBS) and fly ash (FA). The GGBS was used as the source of aluminosilicate materials for the production of geopolymer concrete and the FA was used as an additive to increase the setting time of geopolymer concrete under ambient curing conditions. The GGBS was supplied by the Australian Slag Association [26]. The FA was supplied by Eraring Power Station, Australia [27]. The X-Ray Fluorescent (XRF) was used to analyse the chemical composition of FA and GGBS. The chemical composition analysis of GGBS and FA was conducted in the School of Earth Science at the University of Wollongong Australia. The chemical compositions of GGBS and FA are shown in Table 1. The results of XRF classified the FA as low calcium FA (Type F) according to ASTM C618-08 [28]. The sum of SiO_2, Al_2O and Fe_2O_3 content were higher than 70% of the FA components. The CaO content was less than 8% of the FA components. Coarse aggregate with a maximum size of 10 mm and river sand as a fine aggregate were used in this study.

The roles of alkaline activator solution are to dissolve the reactive portion of the source materials (aluminate (Al) and silicate (Si)) present in GGBS and FA and to provide a high alkaline liquid medium. The alkaline activator solution was a blend of sodium hydroxide

144 (NaOH) and sodium silicate (Na_2SiO_3) solutions. The sodium hydroxide (NaOH) solution
145 was prepared by dissolving caustic soda pellets in potable water. The NaOH solution was
146 prepared 24 hours before casting geopolymer concrete. The Na_2SiO_3 solution included 44.1%
147 solids, 29.4% silicate and 14.7% sodium oxide. The Na_2SiO_3 was supplied by PQ Australia
148 [29]. High range water reducer (Glenium 8700) supplied by BASF Australia [30] was used to
149 improve the workability of the geopolymer concrete.

150 In this study, three types of steel fibres were used: straight micro steel (MIS) fibres, deformed
151 macro steel (DES) fibres and hybrid steel (HYS) fibres. The straight micro steel (MIS) fibres
152 were 6 mm in length and 0.2 mm in diameter with a tensile strength of 2600 MPa [31]. The
153 deformed macro steel (DES) fibres were 18 mm in length and 0.55 mm in diameter with a
154 tensile strength of 800 MPa [32]. The HYS fibres were a combination of MIS fibres and DES
155 fibres. The MIS fibres were supplied by Ganzhou Daye Metallic Fibres Company, China
156 [31]. The DES fibres were supplied by Fibercon Company, Australia [32]. The properties of
157 steel fibres are presented in Table 2. Deformed steel bars of 16 mm diameter were used as
158 reinforcement. Five samples of 16 mm deformed steel bars were tested according to AS1391-
159 2007 [33]. The deformed steel bars have two longitudinal ribs and rows of alternately
160 inclined transverse ribs on both sides of the bars. These ribs contribute positively to the bond
161 strength between reinforcing steel bar and concrete. The average yield tensile strength and
162 corresponding yield strain of the deformed steel bar were 612 MPa and 0.003 mm/mm,
163 respectively.

164 ***2.2 Preparation of concrete sample***

165 A total of ten geopolymer concrete mixes were used to evaluate the effect of the corrosion on
166 the bond between reinforcing steel bars and geopolymer concrete. The bond was evaluated
167 using pull-out tests. The dimensions of the specimens were chosen according to the European

168 Standard pull-out test EN-10080 [34], as shown in Fig. 1. The pull-out test specimens were
169 geopolymer concrete cube specimens with a side length of 160 mm and reinforced centrally
170 with a 16 mm diameter deformed steel bar. The length of the steel bar was 510 mm in order
171 to facilitate the loading of the specimen using the 500 kN Universal Instron testing machine.
172 The bonded length of the tested steel bar in the specimens was five times the diameter of the
173 steel bar (i.e., 80 mm), as shown in Fig. 1. The unbounded length of the steel bar in the
174 specimen was obtained by using a polyvinyl chloride (PVC) pipe at one end of the specimens
175 (Fig. 2). Before mixing of concrete, the deformed steel bars were carefully cleaned and the
176 mass of the deformed steel bars in each specimen was recorded.

177 In this study, three types of moulds were used. Plywood moulds were used for preparing pull-
178 out test specimens. Polyvinyl chloride (PVC) cylindrical moulds of 100 mm diameter and
179 200 mm length were used for preparing concrete cylinders to measure the compressive
180 strength of concrete. Also, PVC cylindrical moulds of 150 mm diameter and 300 mm length
181 were used for preparing concrete cylinders to measure the splitting tensile strength of
182 concrete. Table 3 shows the mix proportion of geopolymer concrete which was adopted from
183 a previous study by Hadi et al. [35]. The dry materials including binder (GGBS+FA), coarse
184 and fine aggregate were first mixed for about 3 minutes. Afterwards, alkaline activator
185 (combination sodium hydroxide with sodium silicate) was slowly added into the mixer
186 together with the superplasticiser and water. The mixing continued for another 5 minutes.
187 The geopolymer concrete mix was poured from the pan mixer into plywood moulds prepared
188 for plain geopolymer concrete specimens. For the fibre reinforced geopolymer concrete
189 specimens, after the dry materials and liquid components were mixed thoroughly, steel fibres
190 were added gradually to the wet mix. Mixing continued until the steel fibres were well
191 dispersed in the geopolymer concrete mixes. Adequate care was taken during the mixing to
192 ensure a uniform distribution of the steel fibres in the geopolymer concrete mixes.

193 The geopolymer concrete was poured into the plywood moulds prepared for the geopolymer
194 concrete specimens. The geopolymer concrete specimens were cast and compacted in three
195 stages. Each stage was internally vibrated using an electric vibrator to remove air voids and to
196 compact the fresh concrete. Afterwards, the geopolymer concrete specimens were kept in the
197 moulds for 24 hours. The specimens were then demoulded and kept under ambient conditions
198 until age of 28 days.

199 ***2.3 Labelling system***

200 In this study, each concrete mix has been identified with an acronym (Table 4). The symbol
201 GC refers to plain geopolymer concrete. The symbols GCMIS and GCDES refer to
202 geopolymer concrete reinforced with straight micro and deformed macro steel fibres,
203 respectively. The numbers (1, 1.5, and 2) afterwards refer to the percentages of steel fibres by
204 volume used in this study. The symbol GCHYS refers to geopolymer concrete with hybrid
205 steel fibres. The GCHYS mixes included combinations of micro steel and deformed steel
206 fibres in different proportions. In this study, the GCHYS mixes included 2% hybrid steel
207 fibres by volume. The GCHYS2a included 0.5% micro steel fibres and 1.5% deformed steel
208 fibres (0.5%MIS+1.5%DES), GCHYS2b included 1% micro steel fibres and 1% deformed
209 steel fibres (1%MIS+1%DES) and GCHYS2c included 1.5% micro steel fibres and 0.5%
210 deformed steel fibres (1.5%MIS+0.5%DES).

211 ***2.4 Accelerated corrosion method***

212 In this study, an electrochemical method was used to accelerate the corrosion of deformed
213 steel bars. The specimens were submerged in a plastic tank filled with sea water for three
214 days before being exposed to an accelerated corrosion process to ensure full saturation of the
215 tested specimen [36]. The accelerated corrosion process was obtained using a direct current

(D.C.) supply providing 30 Volt constant potential at 0 to 4 Amperes (Amp). The direct current was applied to the steel bars embedded in the concrete using the steel bars as the anode. The cathode was made from a galvanised mesh, which was placed around the specimens in the salt solution. The current passed from the steel bars to the galvanised mesh placed inside the salt solution. The end of the steel bar was insulated during the corrosion in order to ensure that only the bonded zone would be corroded. One end of the steel bar was coated with paraffin and wrapped with an insulating plastic membrane. A cushion made from PVC was also used under the specimens to insulate the specimens from the base of the plastic tank. The schematic of the accelerated corrosion set-up is shown in Fig. 3. The experimental setup for the accelerated corrosion process is shown in Fig. 4. The calculated mass loss of the steel bars due to corrosion was calculated according to Faraday's law using Equation (1) [37, 38].

$$Mass\ loss = \frac{t \times I \times 55.847}{2 \times 96487} \quad (1)$$

where t is the duration of exposure (hour) and I is the average current to which the reinforcing bar was exposed. The actual mass loss of the steel bars due to corrosion was calculated using Equation (2) [37, 38].

$$Mass\ loss = \frac{G_0 - G_1}{G_0} \times 100\% \quad (2)$$

where G_o is the initial weight of the steel bars before corrosion and G_1 is the weight of the steel bar at the end of the test. Badawi and Soudki [39] and El Maaddawy and Soudki [40] observed that the use of current density for accelerated corrosion tests provided a similar result estimated by Faraday's law equations, as presented in Equation (1).

2.5 Testing of specimens

The compressive strength tests of geopolymer concrete specimens were carried out according to AS 1012.9-1999 [41] at 28 days. A compression testing machine with a capacity of 1800 kN was used to conduct the compressive strength tests. The splitting tensile strength tests of geopolymer concrete specimens were performed according to AS 1012.10-2000 [42] at 28 days. The specimens were tested at the loading rate of 106 kN/min until the specimen failed.

The concentric pull-out tests were performed for the corroded and non-corroded specimens according to EN-10080 [34]. The pull-out tests were performed using a 500 kN Universal Instron testing machine, as shown in Fig. 5. A specially designed loading frame was used for the pull-out test. The loading frame consisted of two plates in which the bottom plate was clamped to the base of the universal Instron testing machine. The reinforcing steel bar passing through the central hole of the top plate was clamped to the upper head of testing machine (Fig. 5). The specimens were tested up to failure with a displacement controlled loading at 0.1 mm/min. The data were recorded at every two seconds. None of the reinforcing steel bars reached the yield strength during the tests. The axial loads applied by the testing machine were recorded to establish the bond stress. The bond stress was computed from the applied axial loads on the steel bar divided by the surface area of the embedded length of the reinforcing steel bar using Equation (3).

$$\tau = \frac{P}{\pi \times D \times L} \quad (3)$$

where τ is the bond stress, P is the applied load, D and L are the diameter and the bond length of the reinforcing steel bars, respectively.

3. Results and discussions

3.1 Mechanical properties

The average compressive strength and average splitting tensile strength of all concrete mixes are presented in Table 5. For each mix, three specimens for the compressive strength and three specimens for the splitting tensile strength were tested and the average results have been reported. It can be seen in Table 5 that the average compressive strengths and average splitting tensile strengths of GC specimens were lower than the average compressive and average splitting tensile strengths of geopolymer concrete specimens with different types of steel fibre.

The average compressive strength was found to be 41.1 MPa for the GC specimens at 28 days. It can be observed that the increase of MIS fibre content from 0 to 2% by volume, the average compressive strength of the geopolymer concrete increased by 6.3%. With the increase of DES fibre content from 0 to 2% by volume, the average compressive strength of the geopolymer concrete increased by 3.6%. The addition of HYS fibres also increased the average compressive strength of the geopolymer concrete. The enhancement in the average compressive strength of the HYS fibre reinforced geopolymer concrete ranged from 11.9% to 14.8%. Specimens GHYS2b (1%MIS+1%DES) achieved the highest average compressive strength. The increase in the compressive strength of geopolymer concrete with the addition of steel fibre can be attributed to the role of the steel fibre in bridging the cracks, which restrained the initiation and propagation of cracks.

The average splitting tensile strength of the GC specimens was 3.7 MPa for 28 days (Table 5). For the increase of MIS fibre content from 0 to 2% by volume, the average splitting tensile strength of the geopolymer concrete increased by 37.8%. For the increase of DES fibre content from 0 to 2% by volume, the average splitting tensile strength of the geopolymer concrete increased by 43.2%. Finally, the addition of 2% HYS fibre by volume significantly increased the splitting tensile strength. The improvements in the average

284 splitting tensile strength ranged from 51.4% to 64.8%. The highest average splitting tensile
285 strength of the geopolymer concrete was achieved for GCHYS2b (1%MIS+1%DES)
286 specimens. The increase in the splitting tensile strength with the addition of the steel fibre is
287 attributed to the uniform distribution of steel fibre throughout the geopolymer concrete
288 mixes. Consequently, greater efficiencies in delaying the initiation and propagation of cracks
289 were achieved, which improved the splitting tensile strength of reinforced geopolymer
290 concrete.

291 ***3.2 Corrosion and cracking behaviour***

292 In the corrosion process, the electrical potential applied to the positively charged steel bars
293 attracts negatively charged chloride ions from the salt solution into the concrete. When the
294 chloride ions reached the steel bar, the surface of steel bars began to corrode [43]. The
295 specimens were monitored to determine the beginning of the corrosion of steel bars. Figure 6
296 shows the variation of current applied with time in GC and steel fibre reinforced geopolymer
297 concrete specimens.

298 The variation of applied current with time was obtained by calculating the average current at
299 every 24 hour using Digitech QM1575 Multimeter. Figure 6a indicates that the average
300 current in the Specimen GC decreased from 440 mA to 145 mA in 96 hours. Afterwards, the
301 current increased from 145 mA to 180 mA during the next 48 hours. The Specimen GC
302 showed ferrous oxides (brown rust) on the top of the specimens after 240 hours of accelerated
303 corrosion exposure. On the other hand, the average current of the steel fibre reinforced
304 geopolymer concrete specimens decreased for about 96 hours and remained nearly steady for
305 about 500 hours. Afterwards, the average current increased. The MIS fibre reinforced
306 geopolymer concrete specimen showed no sign of brown rust for the same period (after 240
307 hours of accelerated corrosion exposure). As the experiment continued, ferrous oxides

(brown rusts) were observed on the top of the MIS fibre reinforced geopolymer concrete specimens after about 400 hours. The brown rust stains seen on the top of the specimens indicated the beginning of corrosion in the embedded steel bars. Figures 6 (a-c) shows that the trends of the current for the steel fibre (MIS, DES and HYS) reinforced geopolymer concrete specimens were almost similar. The possible reason for the initial decreases in the current was due to the filling of the pores in the concrete by salt and other deposits of the salt water. The increase in the current flow indicated the beginning of the corrosion of reinforcing bar. It can be observed that the initial current readings recorded for the steel fibre reinforced geopolymer concrete specimens were lower than the current readings recorded for Specimen GC. The current readings for geopolymer concrete specimens did not show any significant increase during the accelerated corrosion process. This indicates that the steel fibre reinforced geopolymer concrete demonstrated better resistance against chloride penetration than the Specimen GC.

Initial cracks were observed on the bottom of Specimen GC after about 240 hours of accelerated corrosion. On the other hand, the initial cracks were observed on the bottom of specimens after about 500 hours of accelerated corrosion of steel fibre reinforced geopolymer concrete specimens. The cracking started with increasing the current in the power supply, where the current increased from 1.6 Amp to 3.9 Amp.

At the end of the accelerated corrosion process, all specimens exhibited longitudinal cracks running parallel to the steel bars. The maximum measured crack width was in the range of 0.15-0.25 mm and the crack depth was in the range of 1.5-4.5 mm for the Specimen GC. However, only micro cracks were noticed on the steel fibre reinforced geopolymer concrete specimens. The accelerated corrosion test was stopped at 600 hours. It is apparent that the steel fibre reinforced geopolymer concrete specimens demonstrate better resistance against

chloride penetration compared to the Specimen GC in a corrosive environment. The specimens were removed from the tank for visual inspection and pull-out testing.

3.3 Mass loss measurement

The level of corrosion in the embedded steel bar was determined from the mass loss measurement. The level corrosion in terms of the mass loss of the corroded steel bar due to corrosion were first estimated based on Faraday's law using Equation (1). The electric current and the time of corrosion in the accelerated corrosion test was calculated from Equation (1) based on the calculated mass loss. The accelerated corrosion test was stopped at 600 hours due to the sudden increases in the current reading, which occurred with the cracking at the bottom of the specimens. The actual corrosion levels were measured by the mass loss of the corroded steel bar using Equation (2). At the end of the test, the corroded steel bars were retrieved to determine the mass loss. The corroded steel bars for each specimen were cleaned in order to remove all corrosion residues before weighing. The corroded steel bars were cleaned with deionized water using a metal brush in order to ensure that the steel bars were free from any corrosion residue. Figure 7 shows the steel bars before and after corrosion. The steel bars were weighed and the percentage of mass loss was computed using Equation (2).

The specimens with the highest volume fraction (2%) of MIS, DES and HYS (1%MIS+1%DES) steel fibres together with steel bars before and after corrosion process are shown in Fig. 8. It can be observed from Fig. 8 that the steel bars embedded in Specimen GC noticeably suffered from corrosion damage. On the other hand, the steel bars embedded in steel fibre reinforced geopolymer concrete specimens had lower corrosion effects. The measured corrosion levels and calculated corrosion levels are reported in Table 6. It can be seen from Table 6 that the measured corrosion levels were lower than the calculated corrosion levels. The difference in measured corrosion levels and the calculated corrosion

356 levels can be attributed to the fact that the permeability of the concrete played an important
357 role in the actual level of corrosion. The permeability of the concrete was not included in
358 Equation (1) for the calculation of the theoretical level of corrosion. Although the specimens
359 were immersed in the water for three days prior to the accelerated corrosion process, it would
360 have taken a longer period for the saltwater to reach the steel reinforcing bar [36].

361 Based on the test results, the percentage mass losses of the corroded steel bar were 5.90% for
362 Specimen GC. On the other hand, for the steel fibre reinforced geopolymer concrete
363 specimens, there was a slight mass loss of corroded steel bars after 600 hours of accelerated
364 corrosion testing. Hence, the steel fibre reinforced geopolymer concrete exhibited better
365 corrosion resistance in the marine environment compared to the plain geopolymer concrete.
366 The addition of steel fibres to the geopolymer concrete provided positive effects on the
367 control of the corrosion of steel bar and concrete cracking. Steel fibres in geopolymer
368 concrete led to smaller and more closely spaced cracks, resulting in reduced permeability of
369 the concrete. Also, Specimen GC showed higher mass loss of the corroded steel bar due to
370 the formation of wide cracks on the bottom of the specimens (Fig. 8). The cracks allowed the
371 chloride ions to reach the steel bar quicker and accelerated the rate of corrosion.

372 ***3.4 Bond failure modes***

373 Figure 9 shows the failure patterns of specimens after the pull-out tests. It can be observed
374 that the bond failure of non-corroded specimens was almost similar, except Specimen GC.
375 The failure of the steel fibre (MIS, DES and HYS) reinforced geopolymer concrete
376 specimens occurred by splitting cracks during the pull-out test while the failure of Specimen
377 GC occurred by pull-out failure. The typical splitting cracks of the steel fibre reinforced
378 geopolymer concrete specimens started from the loading end and extended to the free end.

For corroded specimens, the bond failure of Specimen GC was caused by newly generated splitting cracks around the steel bar in addition to the existing corrosion induced longitudinal cracks. This is because of the brittle behaviour of Specimen GC (without steel fibre) due to the corrosion of steel bar. Thus, more cracks generated when sudden loss of bond strength occurred. The steel fibre reinforced geopolymer concrete specimens failed because of the widening of the existing longitudinal crack due to corrosion. The splitting cracks generated or existing longitudinal cracks widened continuously from the loading end to the free end. After the pull-out test, only slip of the steel fibres has been observed.

3.5 Bond versus free-end slip behaviour

Results of pull-out tests are shown in Table 7. The axial load and free-end slip were obtained directly from the 500 kN Universal Instron testing machine. To record the axial load and the free-end slip, an electronic data acquisition system was used.

The behaviour of of bond stress versus free-end slip comprises three stages as shown in Fig. 10. In the first stage (stage I), the bond stress increased until the chemical adhesion is exhausted and slips occurred between the steel bar and the concrete. This stage is limited by the tensile strength of the concrete. The bond stress-slip response remains linear during the first stage. In the second stage (stage II), when the applied axial load increased towards the maximum bond stress, the rate of slip started to increase and the bond stress-slip response became distinctly non-linear. The second stage corresponds to the occurrence of micro-cracking in the concrete specimens. In the last stage (stage III), the specimen reached the maximum bond stress and some longitudinal splitting cracks developed parallel to the steel bar. In this stage, the bond stress decreased with the increase of the slip.

401 Figure 11 shows typical bond stress versus free end slip for non-corroded concrete
402 specimens. It can be seen from Fig. 11 that the maximum bond stress of non-corroded
403 Specimen GC was 16.46 MPa with a corresponding slip of 1.96 mm. The addition of MIS,
404 DES and HYS fibres to the geopolymer concrete increased the maximum bond stress and the
405 corresponding slip (Table 7). The addition of 1%, 1.5% and 2% by volume of MIS fibre
406 increased the maximum bond stress by 28.3%, 32.9% and 38.3%, respectively. The addition
407 1%, 1.5% and 2% by volume of DES fibre increased the maximum bond stress by 24.9%,
408 28.9% and 32.8%, respectively. Also, the addition of MIS and DES fibre increased the slip
409 corresponding to the maximum bond stress noticeably. The slip corresponding to the
410 maximum bond stress of fibre reinforced geopolymer concrete with MIS fibre of 1%, 1.5%
411 and 2% by volume increased by 25.5%, 30.1% and 52.1%, respectively. The slip
412 corresponding to the maximum bond stress of fibre reinforced geopolymer concrete with
413 DES fibre of 1%, 1.5% and 2% by volume increased by 24.5%, 32.7% and 36.7%,
414 respectively. Finally, the addition of hybrid steel fibre increased the maximum bond stress
415 significantly. The improvement of the bond stress ranged from 39% (GCHYS2a) to 65.9%
416 (GCHYS2b). Specimen GCHYS2b achieved the highest bond stress of geopolymer concrete.
417 The slip corresponding to the maximum bond stress of Specimen GCHYS2b was 71.4%
418 higher than the slip corresponding to the maximum bond stress of Specimen GC. It is
419 apparent that the highest increase in the bond stress of geopolymer concrete was achieved by
420 the addition of HYS fibre. This is due to the highest increase in the strength of geopolymer
421 concrete as a result of the addition of HYS fibre, which affected the bond strength of the
422 geopolymer concrete effectively.

423 The bond stress of all the specimens was adversely affected by the corrosion of reinforcing
424 steel bar. The effect of corrosion on the bond stress versus free-end slip are shown in Fig. 12.
425 It can be seen that the bond stress of Specimen GC noticeably dropped due to the loss of

426 interlocking action between the corroded steel reinforcing bar and concrete. The maximum
427 bond stress of Specimen GC was 5.85 MPa with the corresponding slip of 1.35 mm. It was
428 observed that the reduction in the bond stress of Specimen GC was greater than the reduction
429 in the bond stress of the steel fibre reinforced geopolymer concrete specimens under the same
430 corrosion condition. This indicates that the steel fibre reinforced geopolymer concrete
431 specimens exhibited better corrosion resistance compared to Specimen GC. The main reason
432 for the higher losses of the bond stress of Specimen GC might be due to the wide longitudinal
433 cracks that were developed on the specimens, which allowed chloride ions to penetrate
434 quickly into the concrete and accelerate the rate of corrosion.

435 The maximum bond stress of fibre reinforced geopolymer concrete with MIS fibre of 1%,
436 1.5% and 2% by volume increased by 41.9%, 53.5% and 75.38%, respectively, compared to
437 Specimen GC. The strain corresponding to the maximum bond stress of fibre reinforced
438 geopolymer concrete with MIS fibre of 1%, 1.5% and 2% by volume increased by 49.6%,
439 71.8% and 114.1%, respectively. Also, the addition of DES fibre to the geopolymer concrete
440 with 1%, 1.5% and 2% by volume increased the maximum bond stress by about 26.2%,
441 31.3% and 47.5%, respectively, compared to Specimen GC. The strain corresponding to the
442 maximum bond stress of fibre reinforced geopolymer concrete with DES fibre of 1%, 1.5%
443 and 2% by volume increased by 5.2%, 9.6% and 58.5%, respectively. In general, the addition
444 of steel fibre in the geopolymer concrete resulted in an increase in the bond stress. This
445 might be due to the fact that the formation of corrosion on the surface of steel fibres increased
446 the friction between the steel fibre and the geopolymer concrete.

447 Finally, the addition of HYS fibre increased the maximum bond stress significantly. The
448 improvement of the bond stress ranged from 83.8% (Specimen GCHYS2a) to 185.6%
449 (Specimen GCHYS2b). The highest bond stress of geopolymer concrete was achieved by

Specimen GCHYS2b. The slip corresponding to the maximum bond stress was increased by 138.5%. It can be seen from Fig. 12 that the HYS fibre reinforced geopolymer concrete with 1% MIS and 1% DES achieved the highest bond stress for corroded specimens compared to the geopolymer concrete specimens with other types of steel fibres. This can be attributed to the high volume fraction of steel fibres with different shapes and sizes which led to the increase in the availability of fibres crossing the cracked section. Hence, greater efficiency in delaying the growth of micro and macro cracks was obtained. Therefore, the highest improvement in the bond stress of geopolymer concrete specimens with HYS fibres was achieved.

4. Conclusions

An experimental study was carried out to evaluate the effect of corrosion on the bond behaviour of reinforcing steel bars embedded in steel fibre reinforced geopolymer concrete. Based on the results of the experimental investigations, the following conclusions can be drawn:

1. The addition of MIS, DES, and HYS fibres significantly improved the compressive strength and splitting tensile strength of geopolymer concrete mixes. The addition of 2% HYS (1% MIS and 1% DES) fibre by volume achieved the highest compressive strength and splitting tensile strength. All steel fibre reinforced geopolymer concrete specimens failed due to the splitting of concrete along the bonded length of reinforcing steel bar. The splitting failure occurred when the reinforcing steel bar reached the peak axial load, and cracks generated parallel to the applied axial load on the front face of the specimens as the bar pulled out. The failure of control plain geopolymer concrete specimen occurred due to the pull-out of the reinforcing steel bar. The pull-out failure occurred when the reinforcing steel

bar reached the peak axial load and pulled out from the specimen without splitting on any face of the concrete.

2. Due to accelerated corrosion process, the maximum measured cracks width was in the range of 0.15-0.25 mm and maximum measured crack depth was in the range of 1.5-4.5 mm for control plain geopolymer concrete specimen. However, only micro cracks were noticed on the steel fibre reinforced geopolymer concrete specimens.

3. The steel fibre reinforced geopolymer concrete specimens showed good resistance to chloride attack than control plain geopolymer concrete specimen. The addition of steel fibres to the geopolymer concrete significantly enhanced the bond stress and improved the corrosion resistance of the specimens.

4. The bond strength of the tested specimens increased with the increase in the volume content of steel fibres in the geopolymer concrete. The addition of 2% MIS, 2% DES and 2% HYS (1% MIS and 1% DES) fibres by volume achieved an increase in the bond strength by 38.27%, 32.86% and 65.98%, respectively, compared to the control plain geopolymer concrete specimen (Specimen GC). Due to the accelerated corrosion process, the bond strength of fibre reinforced geopolymer concrete with 2% MIS, 2% DES and 2% HYS (1% MIS and 1% DES) fibres by volume reduced by 54.92%, 60.54% and 38.84%, respectively.

The steel fibre reinforced geopolymer concrete exhibited better resistance to corrosion induced damage than plain geopolymer concrete specimens. The addition of steel fibres to the geopolymer concrete provided positive effects on the control of the corrosion of steel bar and concrete cracking. Steel fibres in geopolymer concrete led to smaller and more closely spaced cracks, which reduced the permeability of the geopolymer concrete.

Acknowledgments

The authors would like to express their thanks to the staff of the concrete laboratory of the University of Wollongong, Australia for their kind help. The authors also thank the Australian Slag Association, Wollongong, Australia for providing aluminosilicate materials necessary for this study. The authors would like to acknowledge the Fibercon Company, Australia for providing deformed macro steel fibres required for this study. The first author is grateful for the financial support received from the Iraqi government for his PhD studies.

References

1. Turner LK, Collins FG. Carbon dioxide equivalent (CO 2-e) emissions: a comparison between geopolymer and OPC cement concrete. Construction and Building Materials 2013; 43:125-130.
2. Hardjito D, Wallah SE, Sumajouw DM, Rangan BV. On the development of fly ash-based geopolymer concrete. Materials Journal 2004; 101(6):467-472.
3. McLellan BC, Williams RP, Lay J, Van Riessen A, Corder GD. Costs and carbon emissions for geopolymer pastes in comparison to ordinary portland cement. Journal of Cleaner Production 2011; 19(9):1080-1090.
4. Duxson P, Fernández-Jiménez A, Provis JL, Lukey GC, Palomo A, Van Deventer JSJ. Geopolymer technology: the current state of the art. Journal of Materials Science 2007; 42(9):2917-2933.
5. Al-Majidi MH, Lampropoulos A, Cundy AB. Tensile properties of a novel fibre reinforced geopolymer composite with enhanced strain hardening characteristics. Composite Structures 2017; 168:402-427.
6. Bakharev T. Geopolymeric materials prepared using Class F fly ash and elevated temperature curing. Cement and concrete research 2005; 35(6):1224-1232.
7. Ranjbar N, Mehrali M, Behnia A, Alengaram UJ, Jumaat MZ. Compressive strength and microstructural analysis of fly ash/palm oil fuel ash based geopolymer mortar. Materials & Design 2014; 59:532-539.

524 8. Natali A, Manzi S, Bignozzi MC. Novel fiber-reinforced composite materials based
525 on sustainable geopolymer matrix. Procedia engineering 2011; 21:1124-1131.

526 9. Ng TS, Amin A, Foster SJ. The behaviour of steel-fibre-reinforced geopolymer
527 concrete beams in shear. Magazine of Concrete Research 2013; 65(5):308-318.

528 10. Bernal S, De Gutierrez R, Delvasto S, Rodriguez E. Performance of an alkali-
529 activated slag concrete reinforced with steel fibers. Construction and building
530 Materials 2010; 24(2): 208-214.

531 11. Chen ZJ. Effect of reinforcement corrosion on the serviceability of reinforced
532 concrete structures. Master's thesis, Department of Civil Engineering, University of
533 Dundee, UK, 2004.

534 12. Fu XDDL, Chung DDL. Effect of corrosion on the bond between concrete and steel
535 rebar. Cement and Concrete Research 1997; 27(12): 1811-1815.

536 13. Coccia S, Imperatore S, Rinaldi Z. Influence of corrosion on the bond strength of steel
537 rebars in concrete. Materials and Structures 2016; 49(1-2):537-551.

538 14. Tondolo F. Bond behaviour with reinforcement corrosion. Construction and Building
539 Materials 2015; 93:926-932.

540 15. Abosrra L, Ashour AF, Youseffi M. Corrosion of steel reinforcement in concrete of
541 different compressive strengths. Construction and Building Materials
542 2011; 25(10):3915-3925.

543 16. Okada K, KobayashiI K, Miyagawa T. Influence of longitudinal cracking due to
544 reinforcement corrosion on characteristics of reinforced concrete members. Structural
545 Journal 1988; 85(2):134-140.

546 17. Chen G, Hadi MNS, Gao D, Zhao L. Experimental study on the properties of
547 corroded steel fibres. Construction and Building Materials 2015; 79: 165-172.

548 18. Roque R, Kim N, Kim B, Lopp G. Durability of fiber-reinforced concrete in Florida
549 environments. University of Florida, Tallahassee FL, USA, 2009: 84-85.

550 19. Grubb JA, Blunt J, Ostertag CP, Devine TM. Effect of steel microfibers on corrosion
551 of steel reinforcing bars. Cement and Concrete Research 2007; 37(7):1115-1126.

552 20. Someh AK, Saeki N. The Role of Galvanized Steel Fibers in Corrosion-Protection of
553 Reinforced Concrete. Proceedings of Japan Concrete Institute 1997; 19(1):889-894.

554 21. Sofi M, Van Deventer JSJ, Mendis PA, Lukey GC. Bond performance of reinforcing
555 bars in inorganic polymer concrete (IPC). Journal of Materials Science 2007; 42(9):
556 3107-3116.

557 22. Sarker PK. Bond strength of reinforcing steel embedded in fly ash-based geopolymer
558 concrete. Materials and structures 2011; 44(5):1021-1030.

559 23. Castel A, Foster SJ. Bond strength between blended slag and Class F fly ash
560 geopolymer concrete with steel reinforcement. Cement and Concrete Research
561 2015; 72:48-53.

562 24. Hamad BS, Ali AYH, Harajli MH. Effect of fiber-reinforced polymer confinement on
563 bond strength of reinforcement in beam anchorage specimens. Journal of Composites
564 for Construction 2005; 9(1):44-51.

565 25. Tekle BH, Khennane A, Kayali O. Bond of spliced GFRP reinforcement bars in alkali
566 activated cement concrete. Engineering Structures 2017; 147:740-751.

567 26. Australasian Slag Association, Australasian Slag Association, Wollongong, NSW
568 2500. http://www.asa-inc.org.au/ground-granulated-blast-furnace-slag.php, 2017
569 (accessed on 5 December 2017).

570 27. Eraring Australia, Eraring power station Australia, Level 16, 227 Elizabeth Street
571 Sydney NSW 2000. https://www. originenergy.com.au/about/who-we-are/what we-
572 do/generation.html, 2017 (accessed on 5 December 2017).

573 28. ASTM C618, Standard specification for coal fly ash and raw or calcined natural
574 pozzolan for use in concrete. ASTM International; 2005.

575 29. PQ Australia, PQ Australia Limited, 8/10 Riverside Rd, Chipping Norton NSW 2170,
576 2017 (accessed on 5 December 2017).

577 30. BASF Australia, BASF Australia Limited, 521 Kororoit Creek Rd, Altona VIC 3018.
578 www.basf.com.au, 2017 (accessed on 5 December 2017).

579 31. Ganzhou Daye Metallic Fibres Company. WSF Steel Fiber http://www.gzdymf.com/
580 product/WSF_Steel_Fiber.html, 2017 (accessed on 5 December 2017).

581 32. Fibercon, http://www.fibercon.com.au, 2017 (accessed on 5 December 2017)

582 33. AS 1391-2007. Standard A. Metallic materials-tensile testing at ambient temperature,
583 Australia Standard, Sydney, NSW, 2007.

584 34. EN-10080. Bond test for ribbed and indented reinforcing steel-pull-out test, European
585 committee for standardization, 2005.

586 35. Hadi MNS, Farhan NA, Sheikh MN. Design of geopolymer concrete with GGBFS at
587 ambient curing condition using Taguchi method. Construction and Building Materials
588 2017; 140:424-431.

589 36. Fang C, Lundgren K, Chen L, Zhu C. Corrosion influence on bond in reinforced
590 concrete. Cement and concrete research 2004; 34(11): 2159-2167.

591 37. Yalciner H, Eren O, Sensoy S. An experimental study on the bond strength between
592 reinforcement bars and concrete as a function of concrete cover, strength and
593 corrosion level. Cement and Concrete Research 2012; 42(5):643-655.

594 38. Ma Y, Guo Z, Wang L, Zhang J. Experimental investigation of corrosion effect on
595 bond behavior between reinforcing bar and concrete. Construction and Building
596 Materials 2017; 152:240-249.

597 39. Badawi M, Soudki K. Control of corrosion-induced damage in reinforced concrete
598 beams using carbon fiber-reinforced polymer laminates. Journal of composites for
599 construction 2005; 9(2):195-201.

600 40. El Maaddawy TA, Soudki KA. Effectiveness of impressed current technique to
601 simulate corrosion of steel reinforcement in concrete. Journal of materials in civil
602 engineering 2003; 15(1):41-47.

603 41. AS 1012.9-1999, Methods of Testing Concrete-Determination of the Compressive
604 Strength of Concrete Specimens, Standards Australia Limited, Sydney, 1999.

605 42. AS 1012.10-2000, Methods of Testing Concrete - Determination of Indirect Tensile
606 Strength of Concrete Cylinders (Brasil or Splitting Test), Standards Australia Limited,
607 Sydney, R2014.

608 43. Sahmaran M, Li VC, Andrade C. Corrosion resistance performance of steel-
609 reinforced engineered cementitious composite beams. Materials Journal 2008;
610 105(3):243-250.

611

612

613

614

615

616

617

618

619

620

621 **List of Tables**

629
630
631
632
633
634
635
636
637
638
639
640
641
642
643

644
645
646
647
648
649
650
651
652
653
654
655
656
657
658
659
660
661

662 **List of Figures**

677 Fig. 11 Bond stress versus slip for non-corroded: (a) Specimens GC and GCMIS, (b)

678 Specimens GC and GCDES, and (c) Specimens GC and GCHYS.

679 Fig. 12 Bond stress versus slip for corroded: (a) Specimens GC and GCMIS, (b) Specimens

680 GC and GCDES, and (c) Specimens GC and GCHYS.

681

682
683
684
685
686
687
688
689
690

691 **Table 1**

692 Chemical compositions (mass %) of GGBS and FA.

Component	GGBS	FA
SiO_2	32.40	62.2
Al_2O_3	14.96	27.5
Fe_2O_3	0.83	3.92
CaO	40.70	2.27
MgO	5.99	1.05
K_2O	0.29	1.24
Na_2O	0.42	0.52
TiO_2	0.84	0.16
P_2O_5	0.38	0.30
Mn_2O_3	0.40	0.09
SO_3	2.74	0.08
LOI	NA	0.89

693 LOI: Loss on ignition

694

695
696

Table 2

Properties of steel fibres.

Type of steel fibre	Length (mm)	Diameter (mm)	Tensile strength (MPa)	Density (kg/m^3)
Micro steel (MIS) fibres [31]	6±1	0.2±0.05	>2600	7900
Deformed macro steel (DES) fibres [32]	18	0.55	800	7865

721

722

723

724

725

726

727

728 **Table 3**

729 Mix proportion of geopolymer concrete [35].

Geopolymer mix	Quantity
FA (kg/m^3)	225
GGBS (kg/m^3)	225
Al/Binder	0.35
Aggregate (kg/m^3)	1164
Sand (kg/m^3)	627
Na_2SiO_3/NaOH	2.5
Na_2SiO_3 (kg/m^3)	112.5
NaOH (kg/m^3)	45
NaOH (mole/liter)	14
Superplasticizer (kg/m^3)	22.5
Water (kg/m^3)	45

730

731

732 **Table 4**

733 Test matrix.

Concrete mix	Type of steel fibre	Percentage by volume (%)
GC	Plain geopolymer concrete	0
GCMIS1	Micro steel fibre (MIS)	1 (1% MIS)
GCMIS1.5		1.5 (1.5% MIS)
GCMIS2		2 (2% MIS)
GCDES1	Deformed steel fibre (DES)	1 (1% DES)
GCDES1.5		1.5 (1.5% DES)
GCDES2		2 (2% DES)
GCHYS2a	Hybrid steel fibre (HYS)	2 (0.5% MIS+1.5% DES)
GCHYS2b		2 (1% MIS+1% DES)
GCHYS2c		2 (1.5% MIS+0.5% DES)

734

735

736
737
738
739
740
741
742
743
744
745
746
747
748
749
750
751
752
753
754
755

Table 5

Properties of geopolymer concrete without and with steel fibres.

Concrete mix	Average Compressive Strength (MPa) at 28 days	Average Splitting Tensile Strength (MPa) at 28 days
GC	41.1	3.7
GCMIS1	42.7	4.0
GCMIS1.5	42.8	4.9
GCMIS2	43.7	5.1
GCDES1	41.7	4.6
GCDES1.5	41.9	4.8
GCDES2	42.6	5.3
GCHYS2a	46.0	5.8
GCHYS2b	47.2	6.1
GCHYS2c	46.3	5.6

774 **Table 6**

775 Calculated and measured corrosion level.

Concrete mix	Calculated corrosion (%)	Measured corrosion (%)
GC	6.28	5.90
GCMIS1	3.36	2.25
GCMIS1.5	3.18	2.85
GCMIS2	3.15	2.19
GCDES1	3.68	2.40
GCDES1.5	3.30	2.31
GCDES2	3.22	2.13
GCHYS2a	3.12	2.11
GCHYS2b	2.40	1.94
GCHYS2c	3.14	2.04

776

777

778

779

780

781

782

783

784
785

786

787 **Table 7**

788 Results of pull-out tests for geopolymer concrete mixes.

Concrete mix	Non-corroded specimens		Corroded specimens	
	Maximum bond stress (MPa)	Slip at maximum bond stress (mm)	Maximum bond stress (MPa)	Slip at maximum bond stress (mm)
GC	16.46	1.96	5.85	1.35
GCMIS1	21.12	2.46	8.30	2.02
GCMIS1.5	21.87	2.55	8.98	2.32
GCMIS2	22.76	2.98	10.26	2.89
GCDES1	20.56	2.44	7.38	1.42
GCDES1.5	21.22	2.60	7.68	1.48
GCDES2	21.87	2.68	8.63	2.14
GCHYS2a	22.88	2.94	10.75	2.68
GCHYS2b	27.32	3.36	16.71	3.22
GCHYS2c	23.87	3.06	11.75	2.52

789

790

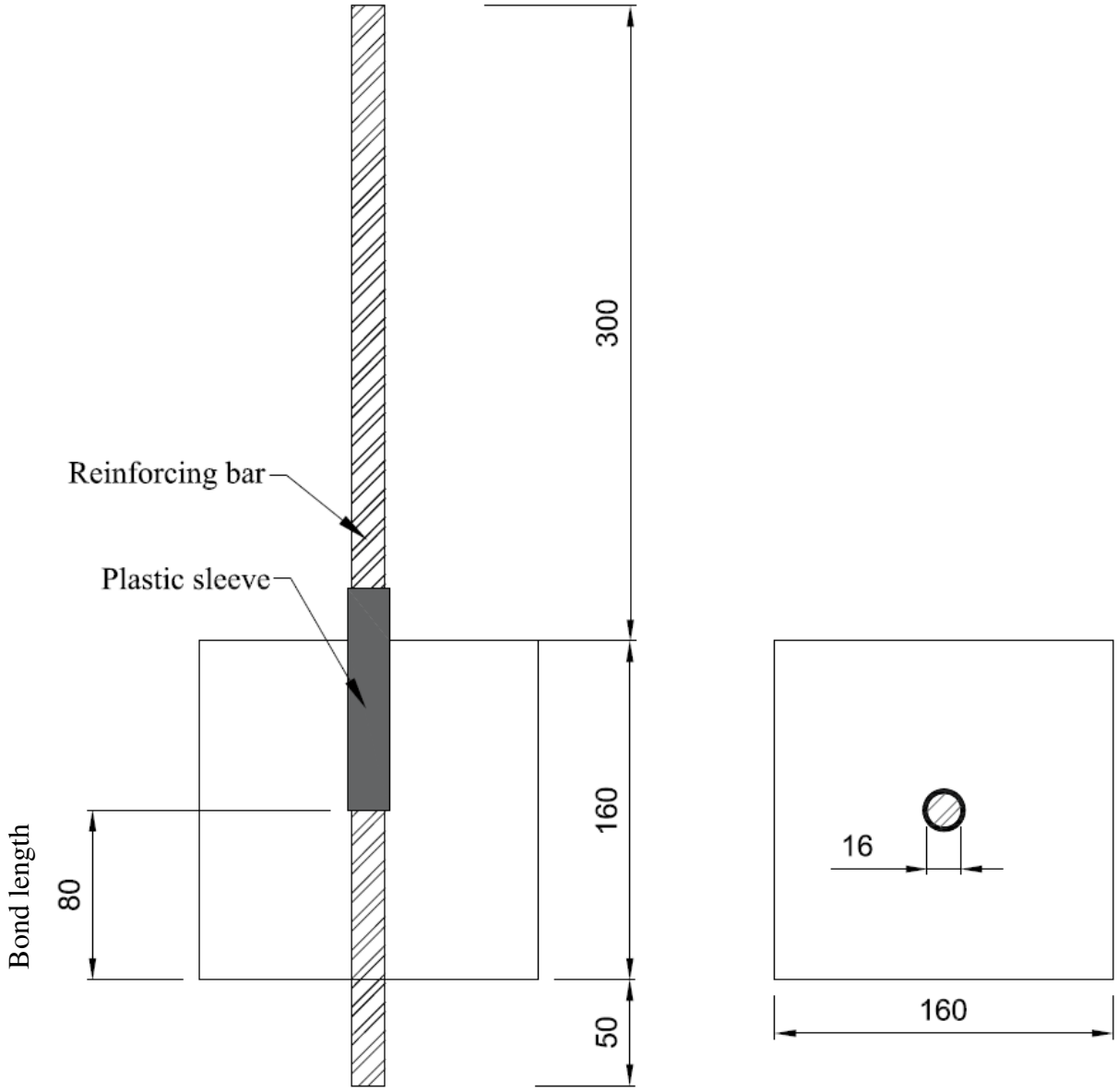

(a) Elevation (b) Plan

Fig. 1. Schematic of the test specimens: (a) Elevation and (b) Plan (Dimensions are in mm).

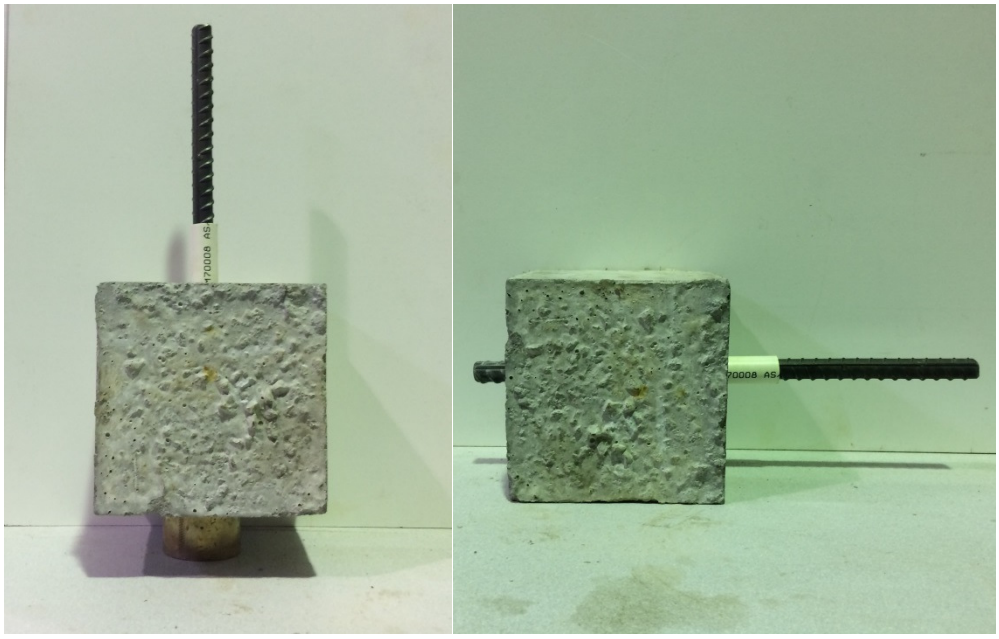

Fig. 2. Pull-out test specimens.

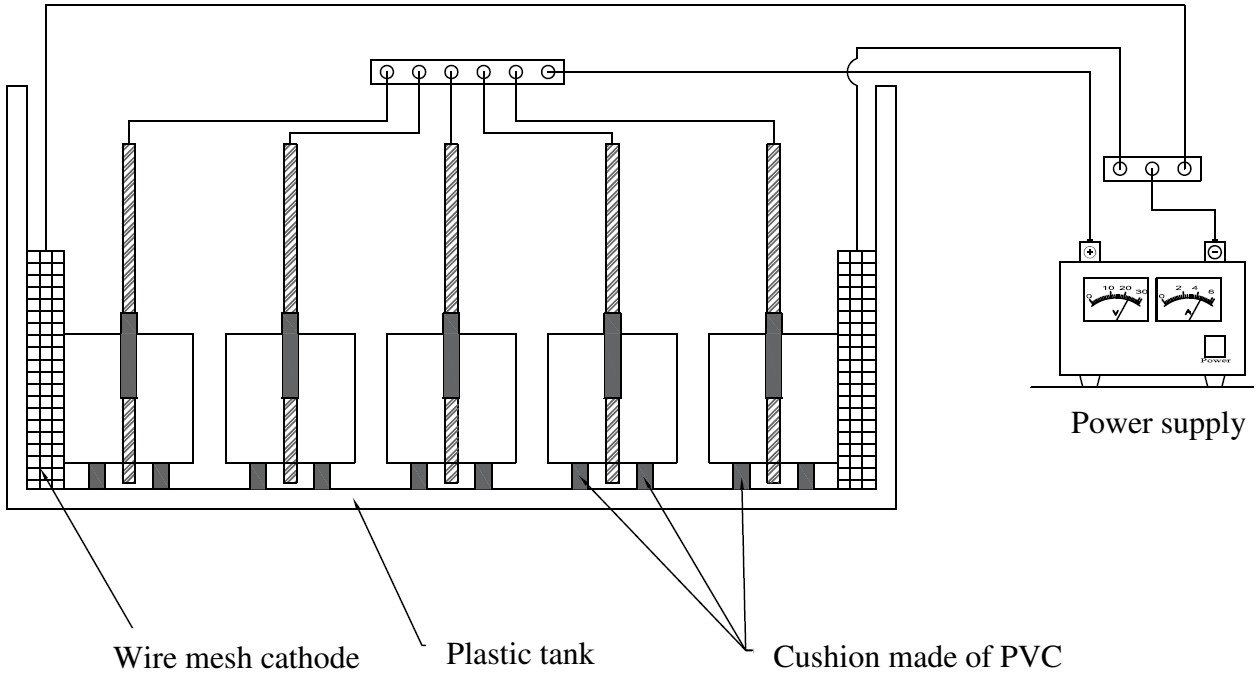

814

815 Fig. 3. Schematic of the accelerated corrosion test set-up.

816

817

818

819

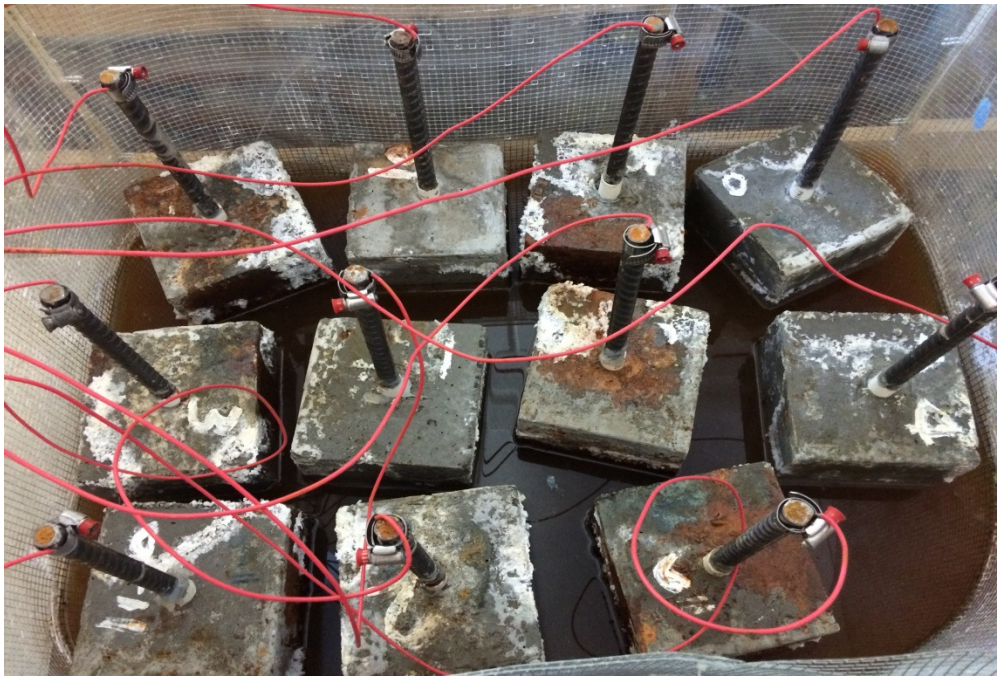

820 Fig. 4. Specimens during accelerated corrosion test.

821

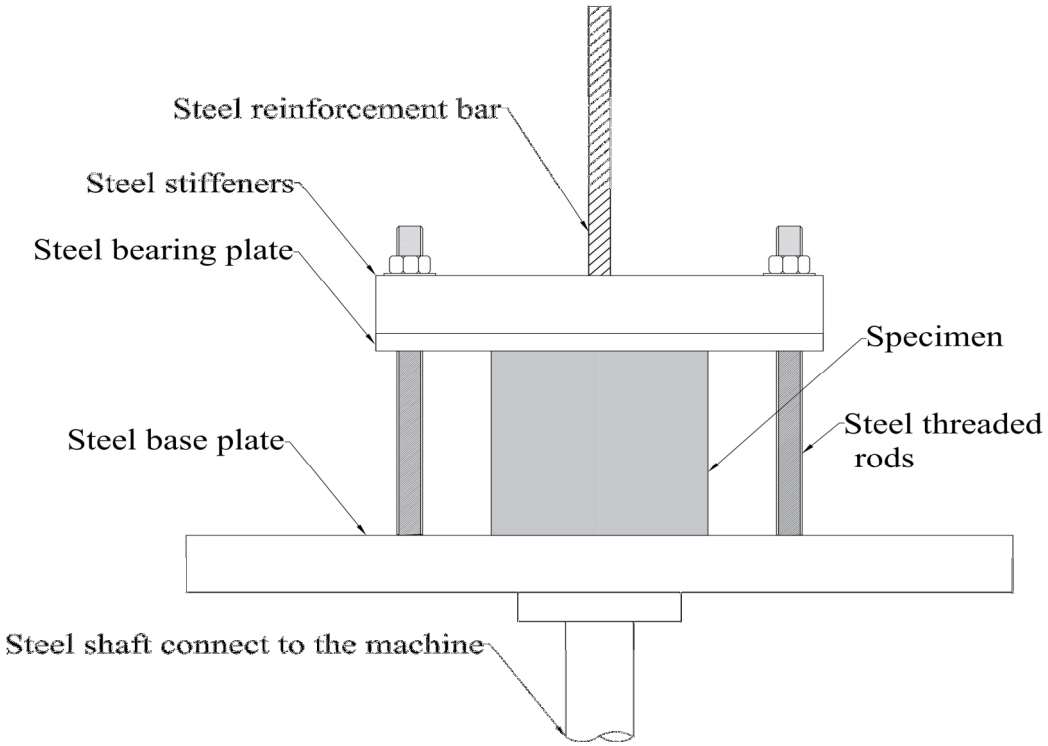

822

(a)

823

824

(b)

825

Fig. 5. Pull-out test: (a) Schematic diagram and (b) Actual setup.

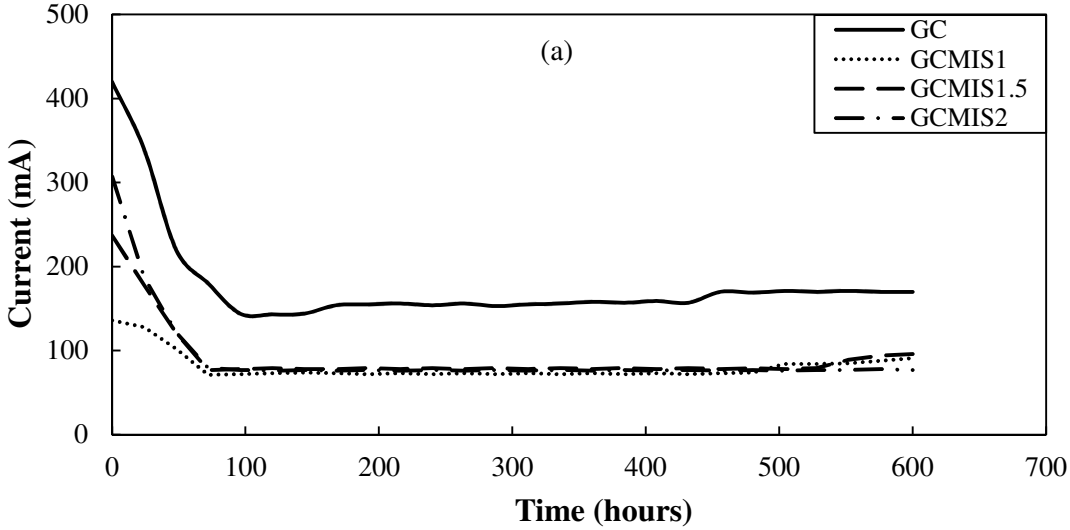

826

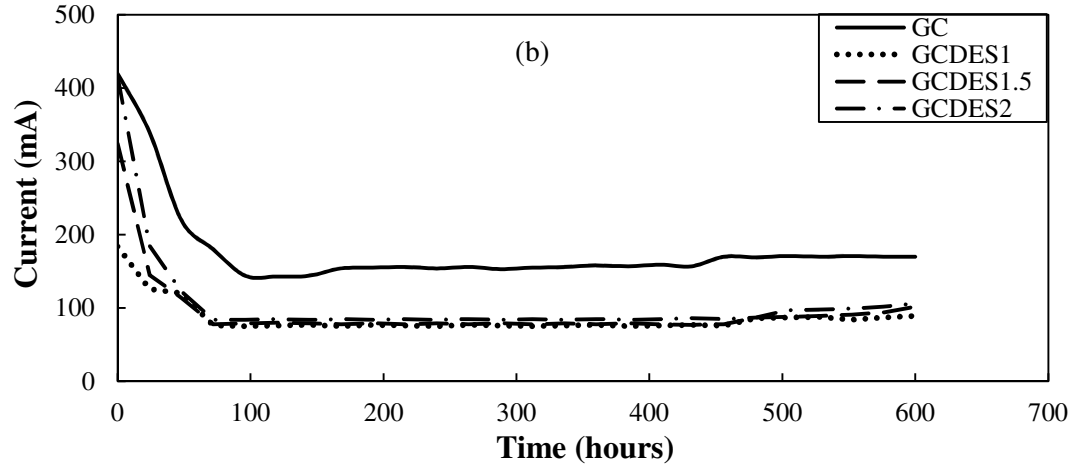

827

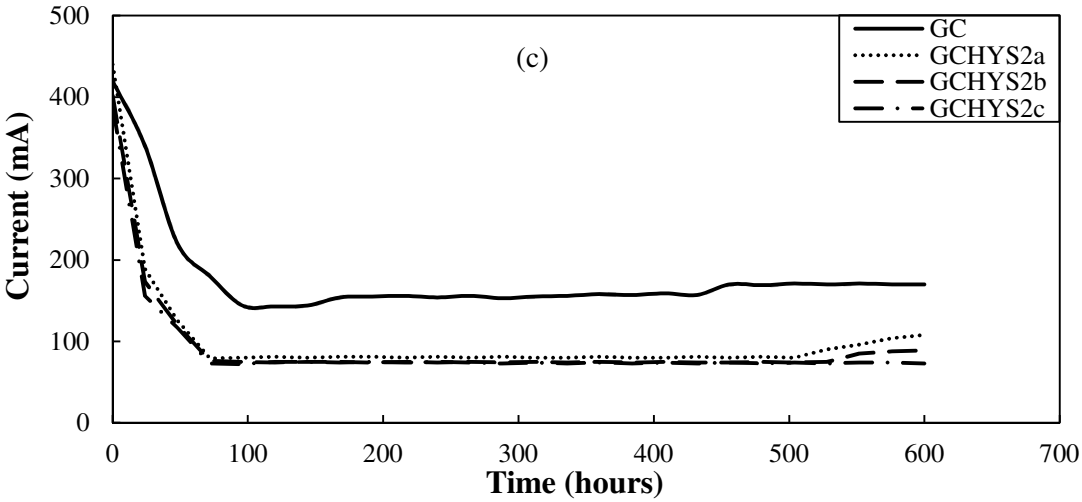

828

829

830 Fig. 6. Variation of current with time: (a) Geopolymer concrete specimens without
831 and with MIS fibres, (b) Geopolymer concrete specimens without and with DES
832 fibres, and (c) Geopolymer concrete specimens without and with HYS fibres.

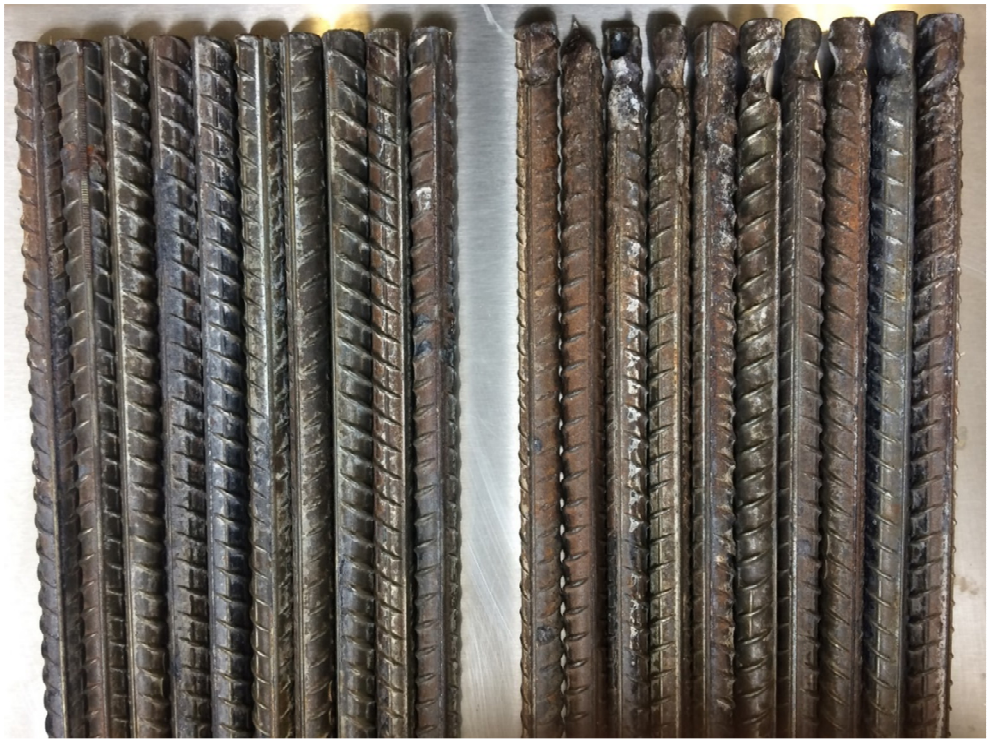

Non-corroded reinforcing steel bars Corroded reinforcing steel bars

Fig. 7. Non-corroded and corroded reinforcing steel bars.

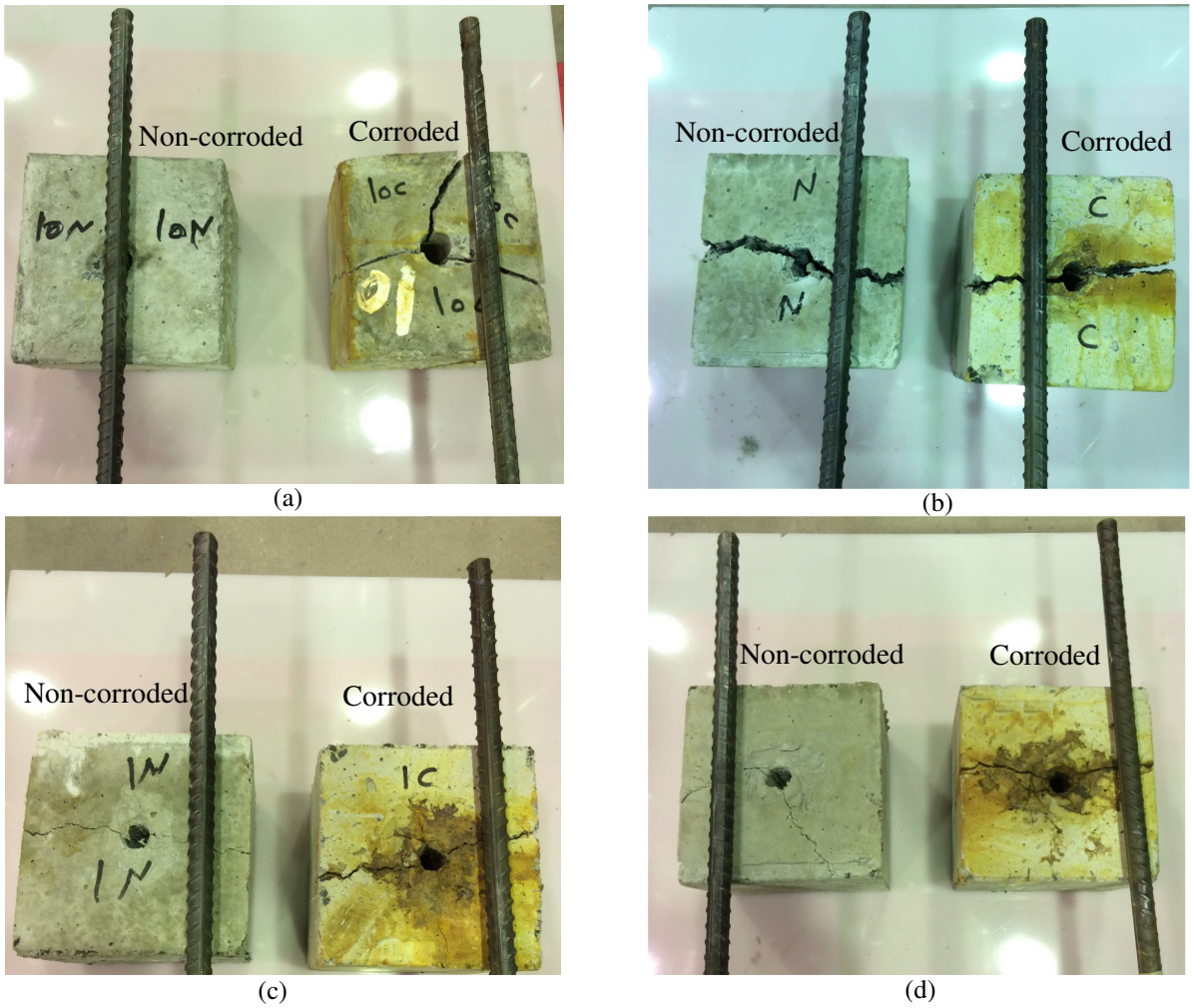

Fig. 8. Specimens before and after the corrosion process: (a) Specimen GC, (b) Specimen GCMIS2, (c) Specimen GCDES2, and (d) Specimen GCHYS2b.

884

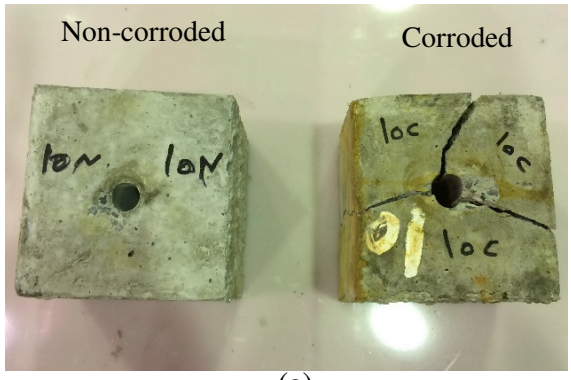

(a)

885

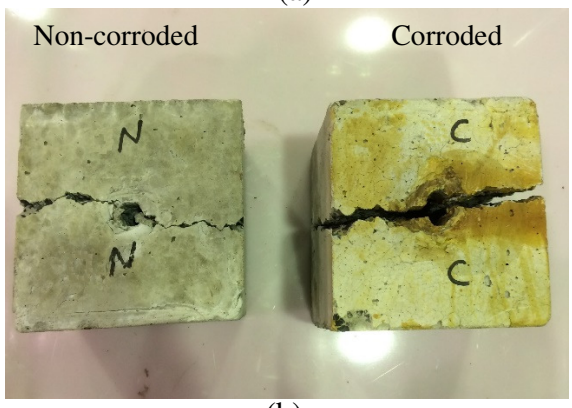

(b)

886

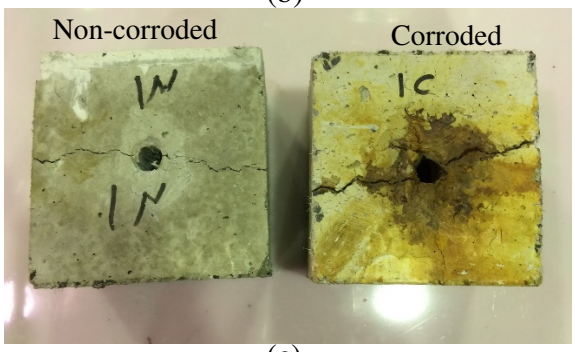

(c)

887

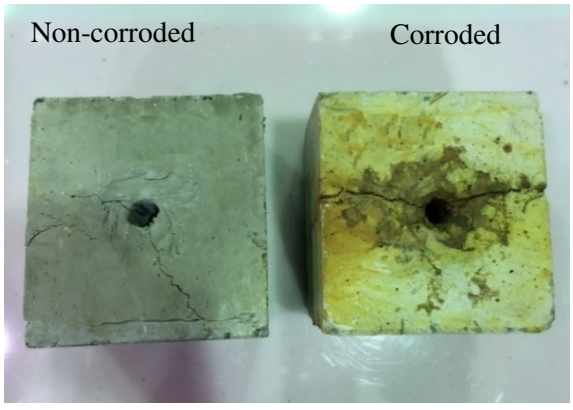

(d)

888

889 Fig. 9. Failure pattern: (a) Specimen GC, (b) Specimen GCMIS2, (c) Specimen GCDES2,
890 and (d) Specimen GCHYS2b.

891

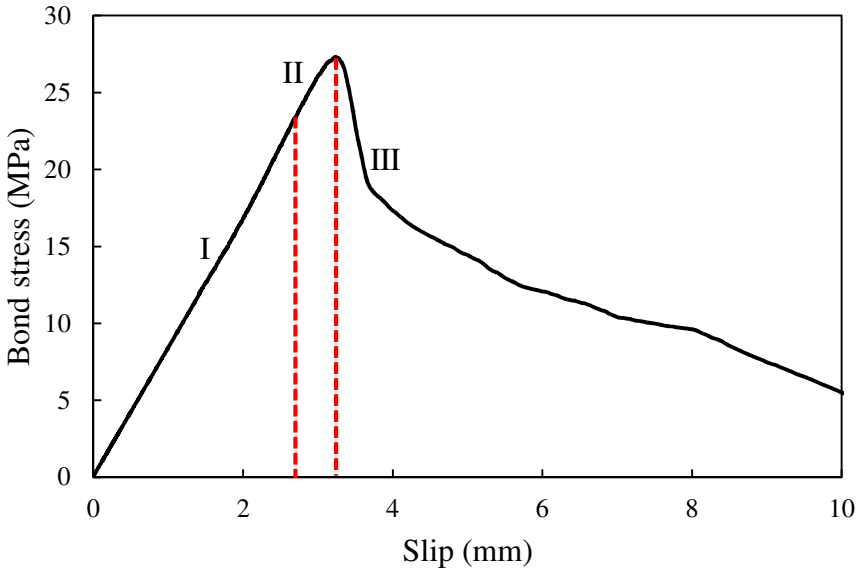

892

893

Fig. 10. General behaviour of bond stress versus slip.

894

895

896

897

898

899

900

901

902

903

904

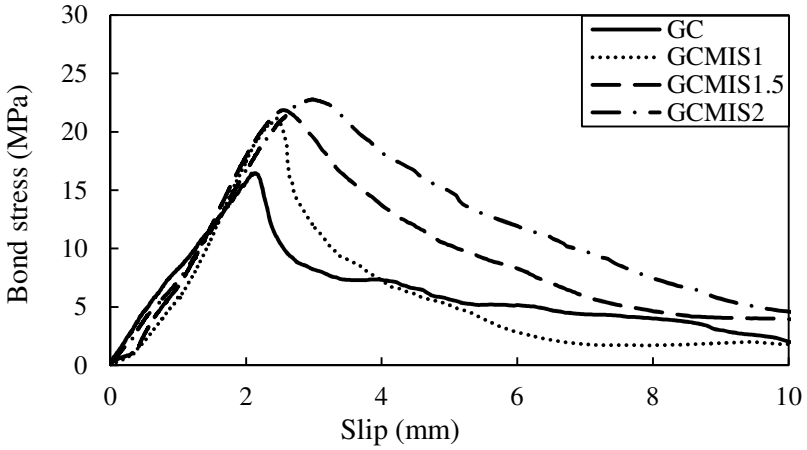

(a) Specimens GC and GCMIS.

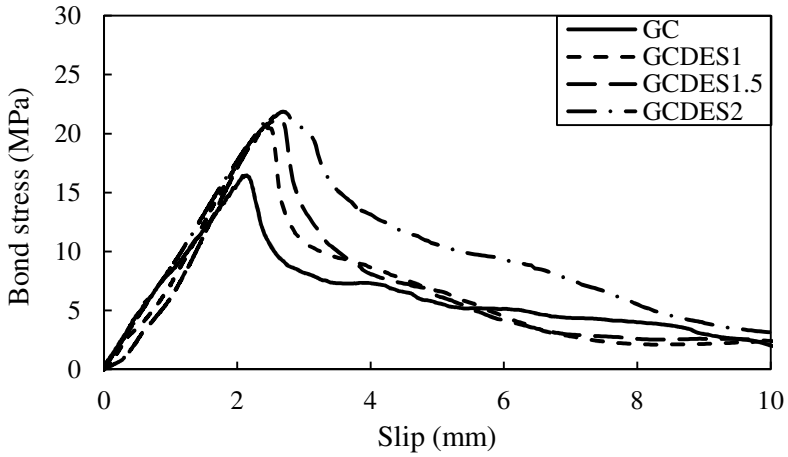

(b) Specimens GC and GCDES.

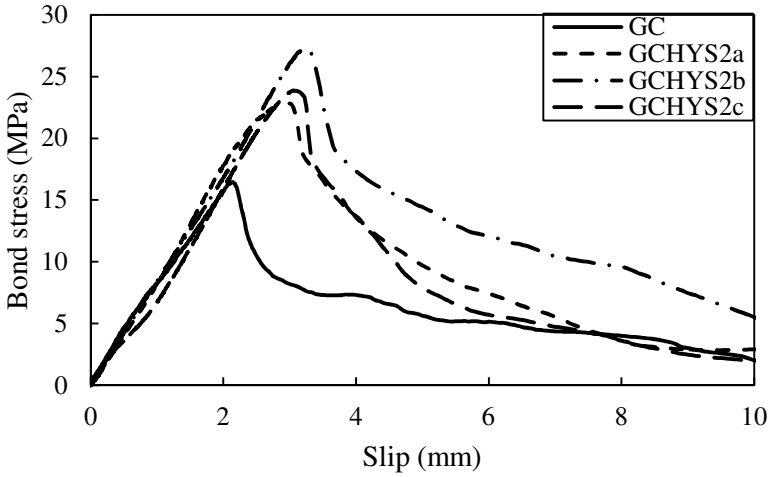

(c) Specimens GC and GCHYS.

Fig. 11. Bond stress versus slip for non-corroded: (a) Specimens GC and GCMIS, (b) Specimens GC and GCDES, and (c) Specimens GC and GCHYS.

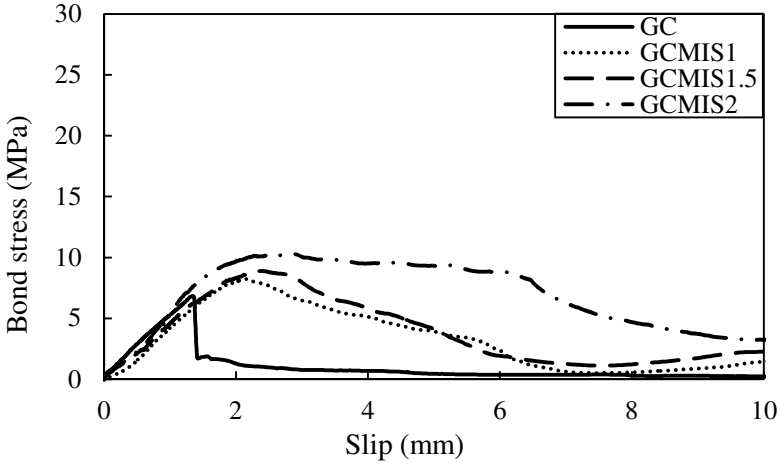

(a) Specimens GC and GCMIS.

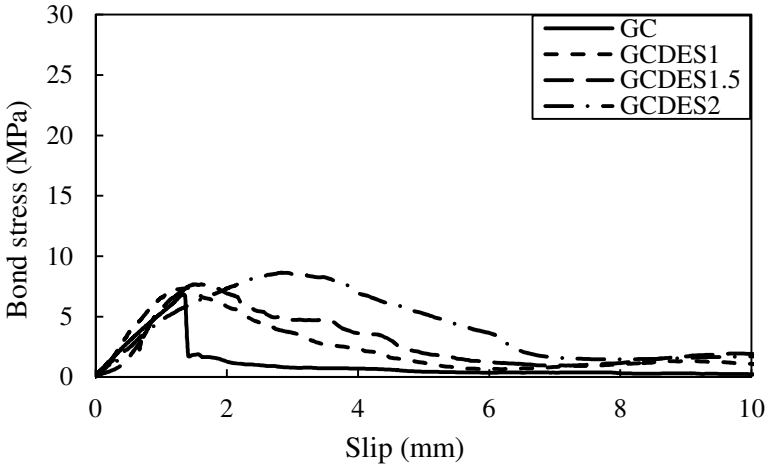

(b) Specimens GC and GCDES.

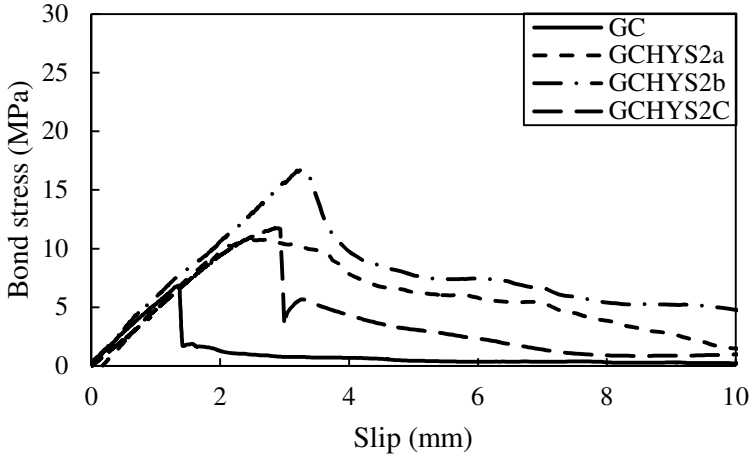

(c) Specimens GC and GCHYS.

Fig. 12. Bond stress versus slip for corroded: (a) Specimens GC and GCMIS, (b) Specimens GC and GCDES, and (c) Specimens GC and GCHYS.